NJC

New Journal of Chemistry

An international journal of the chemical sciences

www.rsc.org/njc

Volume 32 | Number 4 | April 2008 | Pages 557–744

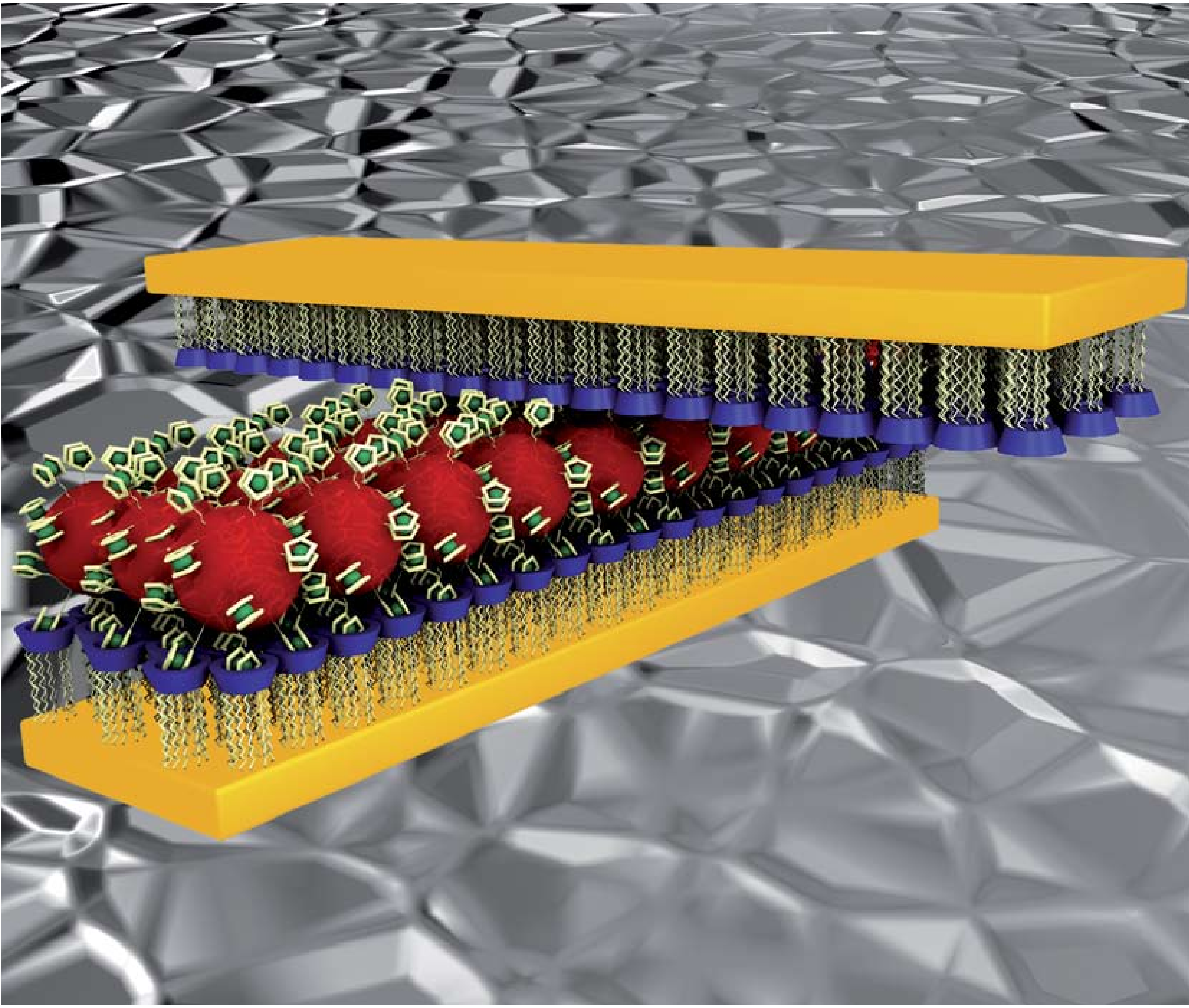

ISSN 1144-0546

RSC Publishing

CNRS CENTRE NATIONAL DE LA RECHERCHE SCIENTIFIQUE

PAPER
Bart Jan Ravoo *et al.*
Preparation of metal–SAM–dendrimer–SAM–metal junctions by supramolecular metal transfer printing

1144-0546(2008)32:4;1-3

Preparation of metal–SAM–dendrimer–SAM–metal junctions by supramolecular metal transfer printing†

Christian A. Nijhuis,[a] Jurjen ter Maat,[a] Satria Z. Bisri,[a] Marcel H. H. Weusthof,[b]
Cora Salm,[b] Jurriaan Schmitz,[b] Bart Jan Ravoo,*[a] Jurriaan Huskens[a] and
David N. Reinhoudt*[a]

Received (in Durham, UK) 24th August 2007, Accepted 11th December 2007
First published as an Advance Article on the web 8th January 2008
DOI: 10.1039/b712979c

Metal–self-assembled monolayer (SAM)–dendrimer–SAM–metal junctions were prepared by a new type of metal transfer printing (mTP) that uses multiple β-cyclodextrin (βCD) host–guest interactions between a metal-coated stamp decorated with a monolayer of host molecules and a substrate which is functionalized with the same host molecules. Metal transfer from the stamp to the substrate is mediated by multivalent guest molecules, immobilized at either the host-functionalized stamp or the substrate, which act as a supramolecular "glue". A βCD SAM was formed at thin Au films that were deposited onto PDMS stamps. Conformal contact of these functionalized PDMS stamps with redox-active monolayers of different generations of ferrocenyl- (Fc-) and biferrocenyl- (BFc-) terminated dendrimers, or redox-inactive monolayers of adamantyl- (Ad-) terminated dendrimers adsorbed at βCD SAMs ("molecular printboards") resulted in transfer of the Au from the PDMS stamp to the substrate. βCD SAMs at different substrates were used, *e.g.* Au and SiO_2. Also transfer of metal to SiO_2 surfaces was possible owing to electrostatic interactions between the positively charged dendrimers and the SiO_2 substrate. Various types of metal patterns were transferred, such as dots, squares or lines with dimensions varying from 5 μm to 50 μm. Lines of 10 μm width and as long as 10 mm could be faithfully transferred.

Introduction

The electronic properties of organic molecules can be designed and tuned by synthesis, and, therefore, they are attractive candidates as active components in a variety of electronic devices, such as organic light emitting diodes,[1] solar cells,[2] and organic field effect transistors (OFETs).[3] OFETs can be applied in identification tags, smart cards, and display drivers. The preparation of molecular devices by means of self-assembly and supramolecular chemistry is a promising method to obtain relatively complicated functional structures that are difficult to prepare in large numbers by other techniques. Of particular interest in molecular electronics are redox-switchable molecules or supramolecular complexes which trigger a difference in conductive states. For instance, self-assembled monolayers (SAMs) of catenanes,[4] rotaxanes,[5] π-conjugated molecules,[6] and transistion metal complexes[7] have been incorporated into devices.

The preparation of organic electronic devices by conventional photolithography requires expensive and elaborate equipment, high temperatures, and/or wet etch chemistry. These may cause degradation of the relatively fragile organic molecules. For these reasons new fabrication techniques, *e.g.* molding, printing, and embossing, have been developed which are low cost tools with patterning capabilities over large areas and which do not suffer from the limitations of conventional techniques.[8]

In particular microcontact printing (μCP) is widely used for large area micropatterning. μCP was developed by Whitesides *et al.*[9] μCP relies on a patterned elastomeric stamp (PDMS) from which ink molecules are transferred to a substrate resulting in a patterned SAM at the substrate.[8] In close analogy, metal transfer printing[10] or nanotransfer printing[11] involves the transfer of a thin metal film from the stamp to the substrate. In organic electronics this method can be of use to introduce top electrodes more reliably than by conventional evaporation of metals on top of molecular monolayers. Metal evaporation commonly results in low yields of working devices due to shortcuts that result from damage to the SAMs and/or diffusion of metal through the SAMs. The metal transfer from the stamp to the substrate relies on the formation of covalent bonds between the metal and the substrate during conformal contact. Subsequent removal of the stamp, to which the metal film binds only weakly, transfers the metal. Au films have been successfully transferred from PDMS stamps to thiol-terminated surfaces at silicon[12] and GaAs surfaces.[13] During

---

[a] *Laboratories of Supramolecular Chemistry and Technology and Molecular Nanofabrication, MESA+ Institute for Nanotechnology, University of Twente, P.O. Box 217, 7500 AE Enschede, The Netherlands. E-mail: smct@tnw.utwente.nl; Fax: (+31)53-4894645*
[b] *Semiconductor Components, University of Twente, MESA+ Institute for Nanotechnology, P.O. Box 217, 7500 AE Enschede, The Netherlands*

† Electronic supplementary information (ESI) available: Analytical data of βCD SAMs on Au-coated PDMS stamps. See DOI: 10.1039/b712979c

conformal contact strong thiol–Au interactions between the substrate and the Au film are formed. Other examples rely on gold welding between the Au substrate and an Au film at the PDMS stamp[14] and a surface condensation reaction.[15] Also relatively complex 3D structures have been realized by mTP.[16] To the best of our knowledge, there are only two examples of mTP where noncovalent surface forces were used for directly printing a metal on a variety of polymer films at elevated temperatures.[17] However, the nature of the adhesion forces between the stamp and substrate remained elusive.

Our group has developed the concept of "molecular printboards", which are SAMs of molecules containing recognition sites to which guest molecules can bind by (multivalent) supramolecular interactions. We have prepared well-ordered and densely packed SAMs of β-cyclodextrin (βCD) on gold[18] and on SiO_2.[19] Onto these SAMs a variety of monovalent or multivalent guest molecules was positioned either by adsorption from solution, or by using microcontact printing or dip-pen nanolithography with submicron resolution.[20] The formation of multiple supramolecular interactions between the guest molecules and the βCD host surface enhanced the pattern stability dramatically.[20]

Dendrimers serve as a very versatile class of polyfunctional guest molecules for the reason that the number of end groups can be exactly controlled and are located at the periphery of the molecule.[21] Moreover, dendrimers have been used as nanocontainers,[22] as nanoreactors,[23] for molecular recognition,[24] as drug carriers,[25] and in catalysis[26] and nanofabrication,[27] making this class of molecules particularly interesting to immobilize at surfaces and to incorporate in devices. Recently, we reported the immobilization of adamantyl- (Ad-),[28] ferrocenyl- (Fc-)[29] and biferrocenyl- (BFc-)[30] functionalized poly(propylene imine) (PPI) dendrimer guest molecules of generations 1 to 5 containing 4 to 64 end groups from aqueous solutions at the molecular printboard by forming multiple host–guest interactions. The higher generations of dendrimers are valuable for nanofabrication, owing to the formation of kinetically stable, multivalent assemblies at the host surface.[31] Furthermore, dendrimers decorated with redox-active Fc moieties have been employed in molecular recognition[32] and electrochemically controlled host–guest complexation.[33] The dendrimers only interact *via* a few end groups with the host surface[29] and many non-interacting end groups are available. We have shown that these end groups can be used to bind βCD-coated gold nanoparticles in a layer-by-layer fashion.[34] Of particular interest in molecular electronics are the dendrimers equipped with redox-active Fc and BFc end groups. We have demonstrated that these redox-active dendrimers bind multivalently to the molecular printboard, but that the host–guest interaction is sensitive to the redox state of the Fc (Fc or Fc^+)[29] and the BFc (BFc, BFc^+ or BFc^{2+})[30] moieties. Recently, we also showed that Ad-functionalized dendrimers loaded with a Au nanoparticle adsorbed at

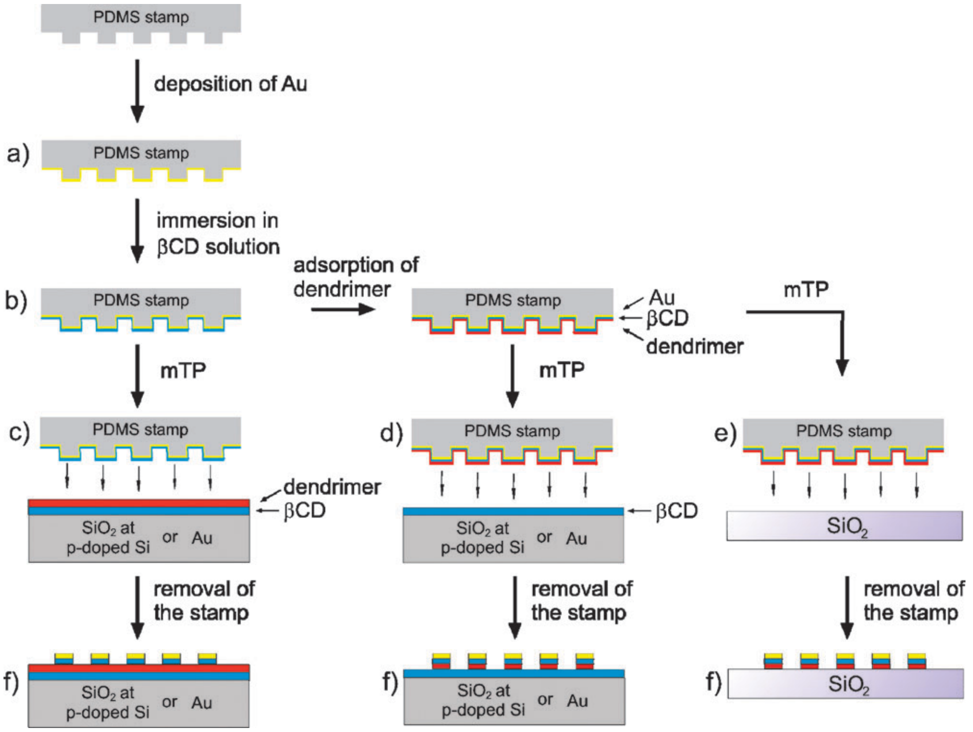

Fig. 1 Schematic illustration of supramolecular mTP: (a) coating the stamp with a layer of 30–40 nm Au; (b) formation of a βCD SAM at the metal stamp by immersion in an ethanolic solution of the βCD adsorbate; (c–e) contacting the stamp with a substrate with a βCD SAM at Au or at SiO_2 at a p-type Si-wafer, at which dendrimers are adsorbed to induce host–guest chemistry (c), or adsorption of dendrimers at the stamp by immersion in an aqueous solution of the dendrimers followed by contacting the stamp with a substrate with only a βCD SAM (d), or with a SiO_2 surface in electrostatic mTP (e); (f) removal of the stamp resulting in transfer of the Au from the stamp to the substrate because the host–guest interactions or the electrostatic interactions are stronger than the inherently weak Au–PDMS interactions. Red: Fc SAM, yellow: Au, and blue: CD SAM.

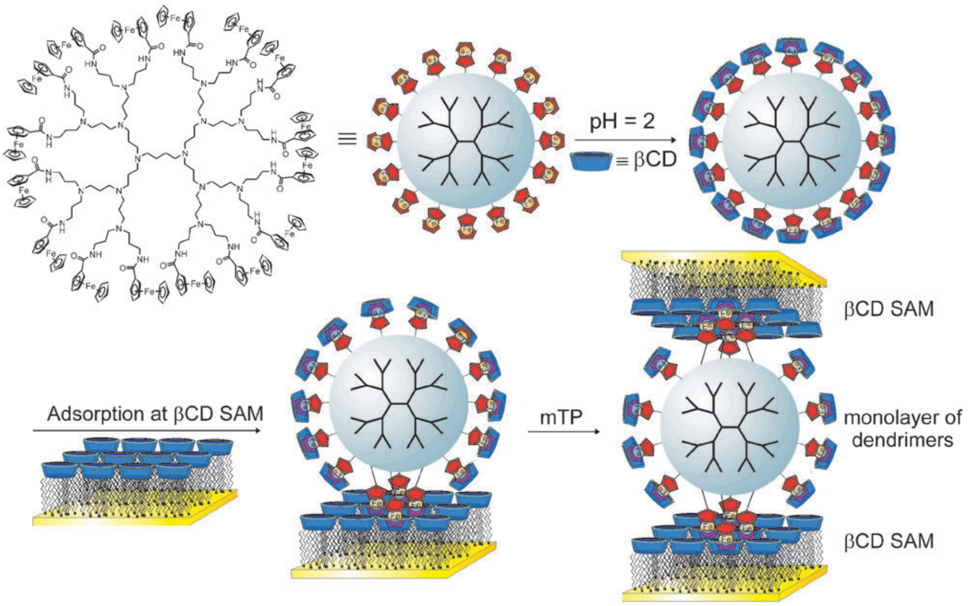

Scheme 1 Schematic illustration of the supramolecular chemistry involved in the preparation of the metal–SAM–metal junctions shown for G3-PPI-$(Fc)_{16}$ on gold: complexation of the dendrimers to βCD resulting in water-soluble assemblies (top); adsorption at the molecular printboard (bottom left), and supramolecular mTP (bottom right).

the molecular printboard display Coulomb staircase behavior under ambient conditions.[35]

This paper describes the preparation of metal–SAM–dendrimer–SAM–metal junctions consisting of Au–βCD SAM–monolayer of dendrimers–βCD SAM–Au (or SiO_2). These multi-component junctions are prepared by mTP mediated by multivalent dendrimers to facilitate the metal transfer from βCD host-functionalized Au stamps to the host-functionalized substrates. Different types of dendrimers were used, namely dendrimers with redox-inactive Ad moieties, and redox-active Fc and BFc end groups, and of generations ranging from G1 (4 end groups) to G5 (64 end groups).

Results and discussion

Supramolecular metal transfer printing

A uniform layer of Au of 30–40 nm was deposited by electron beam evaporation at patterned PDMS stamps (Fig. 1). Immediately after Au deposition the stamps were immersed into an ethanolic solution of heptathioether β-cyclodextrin in order to form a βCD SAM at the thin Au film. After 16 h at 60 °C the stamps were rinsed with 3 cycles of ethanol and dried in a stream of N_2. The presence of the βCD SAM was confirmed by FT-IR, XPS and contact angle measurements on flat stamps and the results were comparable to those found for βCD SAMs on solid Au substrates.[18] Analytical data are available as Electronic Supplementary Information†. It is essential that prior to metal deposition the stamps are ultrasonicated for at least 2 to 3 h in ethanol to remove unreacted oligomers. These are highly mobile and readily diffuse to the surface influencing the stamp surface properties.[36] It has been suggested that low molecular weight PDMS facilitates surface diffusion of the Au atoms during evaporation resulting in discontinuous metal films with large grain sizes.[10] In our study the stamps were kept in ethanolic solutions at elevated temperatures at which low molecular weight PDMS is highly mobile and also segmental motion of the polymer chains may cause instability of the thin Au films.[37] Rippling or buckling of the metal film at stamps due to temperature changes were not observed under these conditions.[38] The evaporation rate is crucial in order to obtain stable Au films that are able to withstand all further manipulations, but do not adhere too strongly with the PDMS stamp. Evaporation rates on the order of 0.6–1.0 Å s^{-1} gave optimal thin metal films for mTP. At low deposition rates the Au atoms may be engulfed by the polymer leading to metal films that strongly interact with PDMS,[39] while at high deposition rates rapid nucleation and metal film growth resulted in unstable Au films.[40] Moreover, high deposition rates may also cause significant heating and deformation of the stamp. It has been reported that Au films at stamps thinner than 20 nm have high sheet resistances due to the presence of low molecular weight silicone which promotes coalescence of Au.[10] For this reason, the stamps were coated typically with 30–40 nm Au to ensure that the metal–SAM–metal junctions prepared by mTP consist of conductive and continuous Au top electrodes.

At βCD SAMs on different substrates (Au or SiO_2), redox-active dendrimers were adsorbed from aqueous solutions (Scheme 1): Fc PPI dendrimers of generations 1 to 5 with 4 to 64 end groups,[29] generations 1 to 3 of the BFc dendrimers,[30] G0-PAMAM-EG-$(Fc)_4$,[29] and a redox-inactive G4-PPI-$(Ad)_{32}$.[28,41] The βCD SAM-functionalized stamps were placed in conformal contact with the substrates containing a monolayer of the dendrimers (Fig. 1c). At this stage, the βCD groups at the Au at the stamp may interact with free end groups of the dendrimers at the substrate (Scheme 1). In order to obtain good contact of the functionalized PDMS stamps with the substrate, the stamp was kept in water vapor for a few seconds before printing according to a procedure reported by

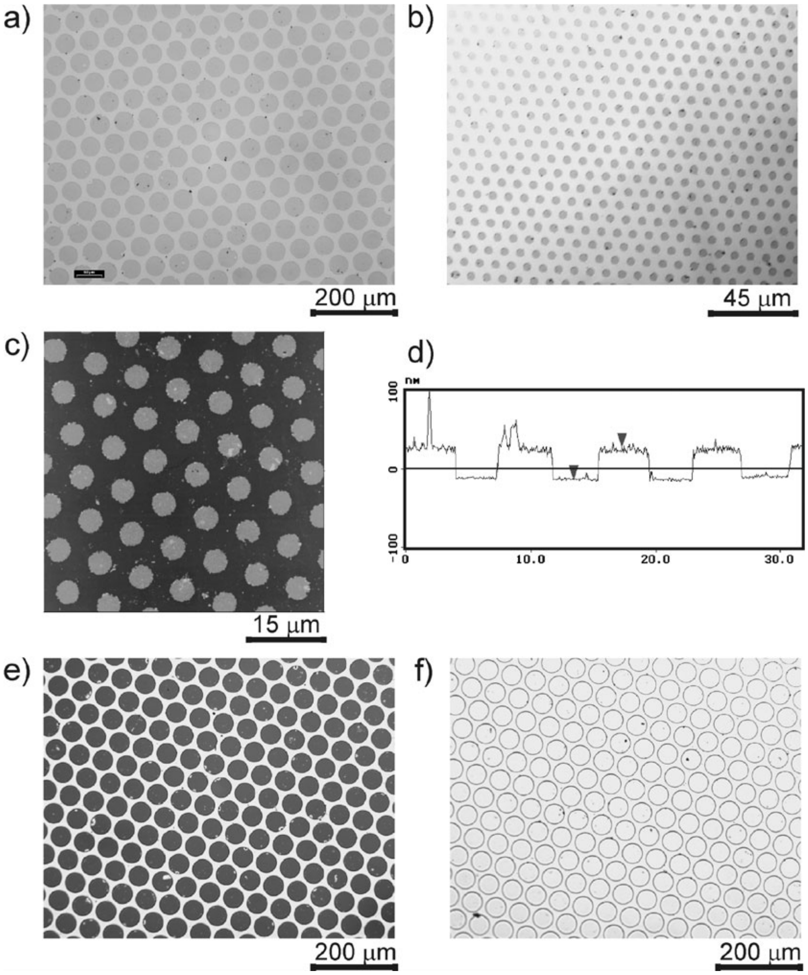

Fig. 2 Optical micrographs of gold patterns printed by supramolecular mTP of: (a) a hexagonal pattern of dots of 50 μm in diameter and a periodicity of 60 μm and (b) dots of 5 μm and a periodicity of 8 μm; (c) AFM image and (d) height profile of a hexagonal pattern of dots of 5 μm and a periodicity of 8 μm; optical micrographs of the stamp before (f) and after mTP (e) to create the pattern shown in (a).

Hoeppener *et al.*[42] The presence of water may favor the formation of host–guest complexes during printing since the host–guest chemistry is essentially a hydrophobic interaction.[43] Additionally, the adsorbed dendrimers can change to an extended conformation upon exposure to water vapor since under relatively dry conditions the dendrimers may collapse and inhibit the formation of host–guest complexes.[44] Thus, due to the thin water film the dendrimers may adopt a fully extended conformation facilitating the formation of a maximal number of host–guest complexes between the functionalized stamp and substrate. Another possible explanation for the improved contact between stamp and substrate after wetting the stamp could be the action of capillary forces. Typical contact times were in the order of 2–3 h after which virtually all the excess water was evaporated and removal of the stamp left the Au behind. Transfer was efficient over large areas. This gave metal–SAM–metal junctions over larger areas (0.5–1 cm^2) consisting of a variety of molecules differing in sizes (ranging from roughly 2.5 nm up to 6 nm) and redox-activity, *e.g.* redox-active Fc dendrimers,[29] electrochemically communicating BFc dendrimers,[30] and redox-inactive Ad dendrimers. Moreover, a variety of structures could be transferred, *e.g.* lines, dots, and squares, of various sizes. Squares and hexagonal patterns of dots ranging from 4 μm to 50 μm in diameter could be transferred, as well as lines of 10 μm width and 10 000 μm long. No significant differences in the effectiveness of mTP were observed using the different types of dendrimers or generations at βCD SAMs at Au or SiO_2 substrates.

Optical micrographs and AFM images of the stamps and the substrates (Fig. 2) clearly show the selective transfer of the metal structures. Optical micrographs of the stamps before and after transfer showed that metal transfer took place exclusively where the stamp made conformal contact with the substrate and not in between the dots (Fig. 2e). AFM showed that the height of the featμures was 40 nm which is in agreement with the metal thickness deposited at the stamp. AFM images revealed that the r.m.s. roughness at the transferred metal structures was in the order of 1.3 nm. In between the structures a somewhat lower r.m.s. roughness of 0.8 nm was found. This indicated that the transferred structures interacted with the underlying surface and completely prevented buckling of the metal film. The somewhat higher surface roughness at the structures could be due to the fact that in between the structures a soft surface was measured (*i.e.* the βCD SAM with adsorbed dendrimers). XPS data revealed

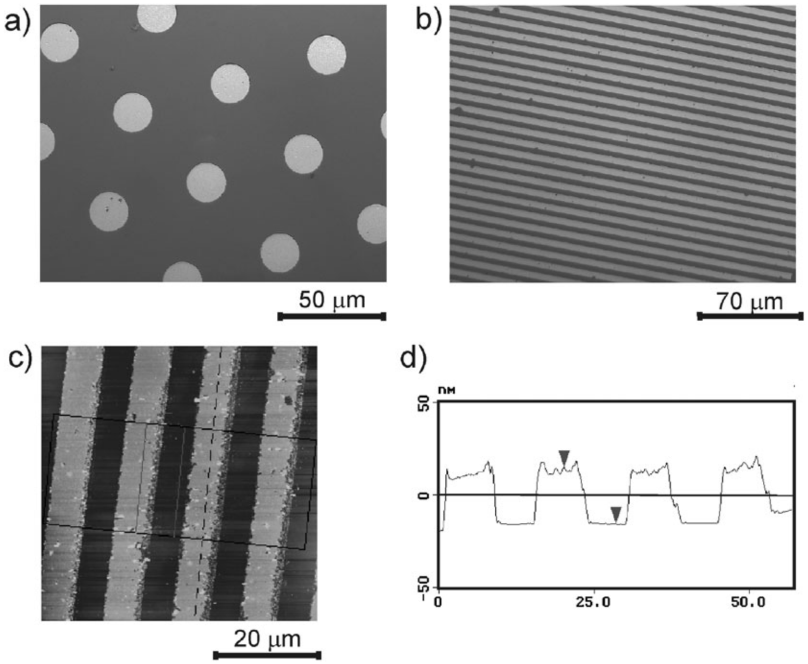

Fig. 3 (a) Optical micrographs after electrostatic mTP of hexagonal patterns of dots (20 μm with a periodicity of 50 μm) and (b) lines of width 10 μm (with a periodicity of 15 μm); (c) AFM image of the same line structures; (d) height profile of the line structures.

only trace amounts of Si at the features indicating that the Au–PDMS interaction is low and that no PDMS was transferred of the stamp during mTP and/or that unreacted PDMS oligomers were efficiently removed during ultrasonication of the stamps.

As stated above, a thin water film was required in order to induce good conformal contact between the stamp and the surface. Therefore, mTP was carried out in the absence of dendrimers in order to study the influence of the thin water film on the printing process. Some structures were transferred despite the fact that no specific host–guest complexes were formed indicating that capillary forces are sufficient for some transfer, but the efficiency of the transfer was dramatically decreased. Subsequent brief ultrasonication (60 s) of the stamps in water resulted in an effective removal of the transferred structures while in the case of the dendrimers the structures remained intact, apart from the edges being slightly damaged. These observations strongly suggest that multiple specific host–guest interactions are essential for effective transfer and stable structures. However, the dendrimer sandwich structures did not withstand the ''scotch tape test''. Rogers *et al.* reported that structures prepared by covalent surface forces withstand the scotch tape test.[12–13,15] This difference may reflect the weaker nature of supramolecular binding compared to covalent binding.

In the fabrication of structures with dendrimers in the metal–SAM–metal junctions, but not in between the structures, the dendrimers were adsorbed on the functionalized stamps instead of on the solid substrate (Fig. 1d). Supramolecular mTP was performed at βCD SAMs at Au or SiO_2. The metal transfer was equally effective. A dendrimer with all end groups interacting with the host surface, *e.g.* G0-PAMAM-EG-$(Fc)_4$,[29] also showed effective mTP. The fact that mTP is still possible indicates that the end groups of this dendrimer interact with the host surface at the stamp. It is well known that βCD-Fc inclusion complexes are dynamic and thus the formation of host–guest complexes of G0-PAMAM-EG-$(Fc)_4$ with the two host surfaces simultaneously is still possible. The number of interactions is also dependent on the effective concentration of host molecules at the surface.[45] Thus, the βCD SAM at the stamp is sufficiently densely packed to obtain metal–SAM–metal structures even when using dendrimers with a small number of end groups.

Electrostatic metal transfer printing

In addition to mTP at a βCD-SAM, mTP at a bare SiO_2 surface was performed with Fc PPI dendrimers of generations 4 and 5, and with G4-PPI-$(Ad)_{32}$, adsorbed at the functionalized Au-coated PDMS stamp (Fig. 1e). The stamps were placed in conformal contact with a freshly cleaned SiO_2 substrate and water vapor was used to induce good conformal contact between the stamp and the surface. Upon subsequent removal of the stamp, mTP proved to be highly effective as is illustrated by the optical micrograph and AFM image of the structures shown in Fig. 3. The lines are 32 nm in height corresponding to the metal thickness deposited at the stamp (Fig. 3d). In this case, transfer was accomplished *via* electrostatic interactions since the SiO_2 surface is negatively charged and the PPI dendrimers are positively charged. A control experiment without dendrimers gave virtually no transfer indicating that indeed the electrostatic interactions of the dendrimers with the surface are essential to facilitate mTP.

A relatively simple way to determine whether the transferred Au features have shortcuts with the underlying Au of the substrate is to perform electrodeposition of Cu (Fig. 4).[46] Under the proper conditions, electrodeposition can only take place if the Au dots have shortcuts or if the monolayer in between the dots has defects. In electrodeposition of Cu, the

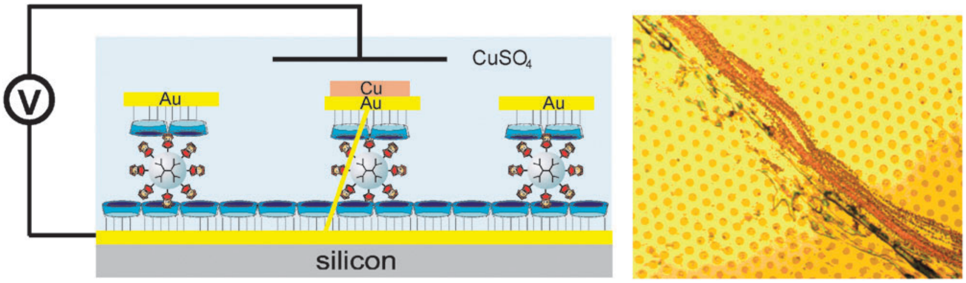

Fig. 4 Schematic illustration of electrodeposition of Cu: the Au at the substrate is used as a working electrode while the reference and counter electrodes are kept in the solution of 10 mM $CuSO_4$ at pH = 2; right: optical micrograph after electrodeposition: virtually no Cu was deposited at the transferred Au features or at the βCD SAM-protected Au in between, a scratch served as an internal reference at which Cu was deposited.

Au layer of the substrate is used as an electrode while the counter electrode is kept in solution together with the Cu^{2+} ions and the reference electrode. The Cu^{2+} ions are only reduced at locations where the electrode is not well protected or where the sandwiches have shortcuts. The aqueous solution contained 10 mM of $CuSO_4$ at pH = 2 and a static potential was applied at −0.7 V for a period of 30 s. At this potential, Cu was deposited at an unprotected Au electrode, but not on βCD SAMs and, therefore, these conditions are suitable to determine whether the structures have shortcuts (Fig. 4, right). Prior to deposition, the sandwich structures (in this case a hexagonal pattern of circular features of 4 μm in diameter transferred using G4-PPI-$(Fc)_{32}$ adsorbed at the substrate) were analyzed by AFM and features of 40 nm high were measured. After applying a potential of −0.7 V for 30 s AFM images and optical micrographs (Fig. 4, left) clearly showed that no Cu was deposited indicating that none of the devices has shortcuts with the underlying Au. As an internal reference, Cu deposition could be clearly observed by optical micrography at an intentionally made scratch.

Electrostatic and supramolecular mTP combined

To demonstrate the potential of supramolecular mTP in the fabrication of more sophisticated structures, mTP was performed at patterned Au substrates. An Au substrate at a Si wafer was patterned by printing octadecanethiol (ODT) followed by immersion in a wet etch solution to remove unprotected Au areas.[47] Next, all organic material was removed by oxygen plasma, which in addition oxidizes the Si surface in between the Au lines. Lines of Au of 10 × 10 000 μm were obtained on which a βCD SAM was deposited. For mTP, Au-coated stamps with a βCD SAM were used with the same line pattern onto which dendrimers, *e.g.* Fc PPI dendrimers of generations 1 to 5, generations 1 to 3 of the BFc dendrimers, or G4-PPI-$(Ad)_{32}$, were adsorbed. Cross-printing (that is ~90° rotation of the stamp with respect to the substrate pattern) gave a grid-like structure since at the crossings mTP is efficient owing to the formation of multiple specific host–guest interactions while in between the crossing mTP is efficient owing to electrostatic interactions of the dendrimers with the SiO_2 surface. An AFM image and an optical micrograph shown in Fig. 5 clearly illustrate that mTP is highly selective using two types of interactions between the stamp and substrate simultaneously to facilitate transfer of the metal film from the PDMS stamp to the substrate. Also here, no differences in mTP were observed using the different types of dendrimers.

Supramolecular junctions

The (I,V)-characteristics of the metal–SAM–dendrimer–SAM–metal junctions can be conveniently measured using cross-bar structures composed of continuous lines (Fig. 5) and/or the structures shown in Fig. 6. The latter structures were obtained by mTP of bars of 25 μm × 10 μm with gaps of 15 μm. The rectangles have an overlaid structure and the top electrodes were introduced by 90° rotation of the

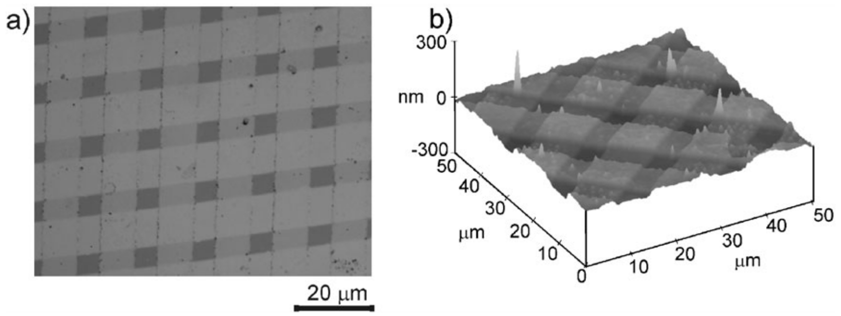

Fig. 5 Optical micrograph (a) and an AFM image (b) of supramolecular mTP on patterned Au substrates on a Si wafer. The Au-coated wafer was patterned with lines of 10 μm wide by microcontact printing a SAM of ODT at the Au-coated wafer followed by a wet etch to remove unprotected gold areas.[47] The ODT SAM was removed in oxygen plasma and a βCD SAM was formed at the pre-patterned Au surface by immersion in ethanolic solution of the βCD adsorbate. Dendrimers were adsorbed on a PDMS stamp with the same line pattern functionalized with a βCD SAM on a thin Au film. The structures were completed by a ~90° cross-print step; the metal was transferred *via* supramolecular interactions at the junctions and *via* electrostatic interactions in between the junctions.

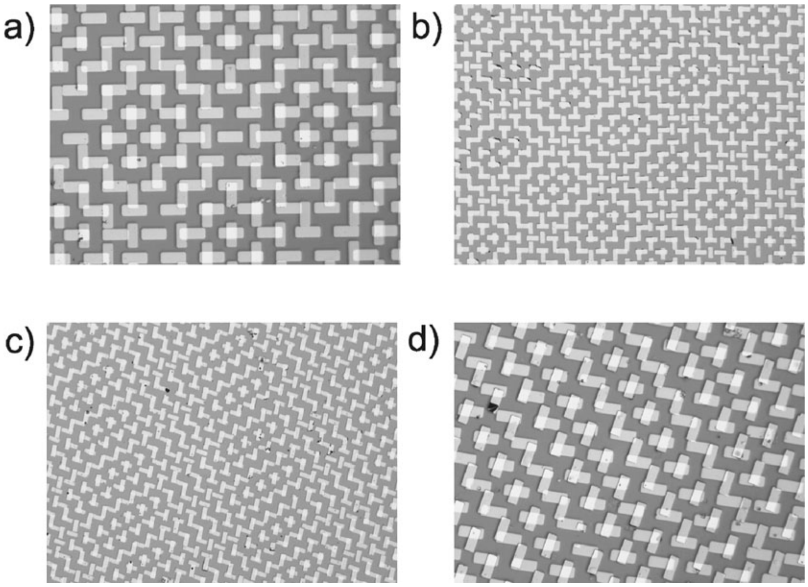

Fig. 6 Optical micrographs of the two-terminal devices prepared by mTP using bars of length 25 μm and 10 μm width. The cross-printing was carried out at 90° (A), 85° (B), 80° (C) and 75° (D).

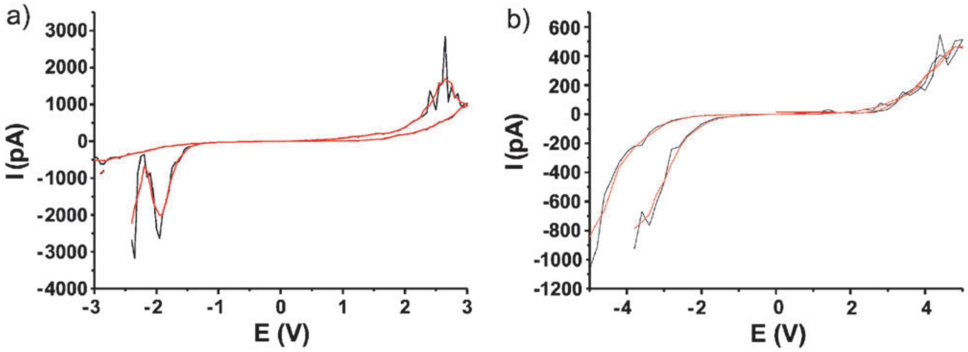

Fig. 7 (*I*,*V*)-characteristics of G4-PPI-$(Fc)_{32}$ and of G5-PPI-$(Ad)_{64}$. The red lines represent smoothed data points.

stamp with respect to the substrate with the same pattern resulting in the structures shown in Fig. 6. Rotation of less than 90° resulted in complex structures, for instance, rotation of 85° (Fig. 6B), 80° (Fig. 6C) and 75° (Fig. 6D) show the change to almost continuous lines of alternating structures.

The (*I*,*V*)-characteristics of the junctions were measured using microneedles in a manually operated probe station under ambient conditions. As a proof-of-concept, Fig. 7 shows (*I*,*V*) measurements for junctions consisting of monolayers of G4-PPI-$(Fc)_{32}$ (Fig. 7A) and G5-PPI-$(Ad)_{64}$ (Fig. 7B). The junctions containing the redox-active Fc dendrimers showed negative differential resistance, *i.e.* a decrease in current while the voltage increases (Fig. 7A). In the case of G5-PPI-$(Ad)_{64}$ (Fig. 7B), no peaks were observed. The NDR peak varied from 2 V and 3 V for the Fc dendrimers and the peak-to-valley ratio of the NDR wave varied from 2 to 5. Currents varied over 2 orders of magnitude, most probably due to defects in the SAM structure and/or filament formations. It is noteworthy that the junction area is 100 μm^2.

NDR has been observed in different experimental settings and molecular electronic devices, but a general explanation for NDR is still under debate.[48] Redox-active monolayers of Fc alkylthiols on Au showed NDR which was related to a resonant tunneling mechanism involving different redox states of the Fc moiety.[49,50] NDR could be attenuated by complexation of βCD to the Fc moieties.[51] There is evidence that NDR could originate from reaction under ambient conditions of the oxidized Fc with oxygen.[52] In the present case, the NDR may be related to the fact that Fc-βCD bond diminishes upon oxidation.[33] This could result in a decrease in currents, hence a NDR. The quantitative analysis and interpretation of the electronic behavior of these supramolecular junctions is the subject of current investigations in our laboratory.

Conclusions

A new type of transfer printing has been introduced based on supramolecular interactions that facilitate metal transfer from a stamp to a substrate. Thin Au films at elastomeric stamps as well as the substrate were functionalized with a βCD SAM. Supramolecular transfer printing was realized by adsorption of multivalent guest molecules that act as supramolecular "glue" at either the stamp or at the substrate. More sophisticated crossbar structures could be prepared on patterned Au substrates on SiO_2 using supramolecular and electrostatic interactions simultaneously.

A variety of metal–SAM–metal structures were constructed by chemical modification of the molecules, *e.g.* Fc-, BFc-, and Ad-functionalized dendrimers, and relatively simple changes in the process steps, *i.e.* dendrimers adsorbed at the stamp or at the substrate. The quantitative analysis and interpretation of the electronic behavior of these supramolecular junctions is the subject of current investigations in our laboratory. The integrated top-down and bottom-up approach to nanofabrication demonstrated here will potentially lead to modular assembly protocols of nanoscale devices by self-organisation.

Experimental section

Materials and methods

The per-6-amino β-cyclodextrin,[53] ferrocenyl[54] and biferrocenyl PPI dendrimers,[30] ferrocenyl PPI dendrimers with tetraethylene glycol tethers[29] and the adamantyl PPI dendrimers[55] were prepared as described previously. All glassware used to prepare monolayers was immersed in piranha solution (conc. H_2SO_4 and 33% H_2O_2 in a 3 : 1 ratio). (**Warning**: piranha should be handled with caution; it can detonate unexpectedly.) Next, the glassware was rinsed with large amounts of Milli-Q water. All adsorbate solutions were prepared prior to use. All solvents used in monolayer preparation were of p.a. grade.

Substrate preparation. At gold

Gold substrates of 20 nm metal thickness with a 2 nm titanium adhesion layer were obtained from SSENS bv (Hengelo, The Netherlands). Gold substrates were cleaned by brief immersion in piranha and the resulting oxide layer was removed by leaving the substrates for 10 min in absolute EtOH. The preparation of a βCD SAM on Au has been reported and the same procedure was used here.[18] Briefly, The substrates were subsequently immersed in the adsorbate solution (0.1–1 mM) for *ca.* 16 h at 60 °C. Next, the samples were removed from the solutions and rinsed thoroughly with chloroform, ethanol, and Milli-Q water.

At silicon

SiO_2 was thermally grown to a depth of 50 nm on four-inch polished, 100-cut, p-doped silicon wafers, and these were cut into 2 × 2 cm^2 samples and used for monolayer preparation. The synthesis of a βCD SAM on SiO_2 has been reported and the same procedure was used here.[19] Briefly, microscope glass slide were oxidized by immersion in boiling piranha (conc. H_2SO_4 and 33% H_2O_2 in a 3 : 1 ratio) for 15 min, rinsed with copious amounts of Millipore water and dried in a stream of N_2. Subsequently, a monolayer was formed by reaction with 1-cyano-11-trichlorosilylundecane. Reduction gave the amine-terminated monolayer which was converted to isothiocyanate-terminated monolayer by reaction with 1,4-phenylene diisothiocyanate. Finally, reaction with per-6-amino β-cyclodextrin gave the host surface.

Dendrimer adsorption

Adsorption of the dendrimers was carried out by immersing a preformed βCD SAM on Au or silicon in an aqueous solution of the corresponding dendrimer–βCD assemblies solutions (0.1 or 1.0 mM in ferrocene functionality in the presence of 11 mM βCD at pH = 2) for at least 3 h. Subsequently the samples were thoroughly rinsed with Milli-Q water (at pH = 2 to ensure full protonation of the amines) and dried in a stream of N_2.

Supramolecular metal transfer printing

Stamps were fabricated by casting a prepolymer of PDMS (DOW Sylgard 184) against a photolithographically patterned silicon master, cured for 20 h at 60 °C, and released at 60 °C. Subsequently the stamps were ultrasonicated in ethanol for 2–3 h and dried in a stream of N_2. The stamps were coated with Au by thermal deposition using a Balzers BAK-600 at deposition rates in the range of 0.6–1 Å s^{-1} at 2×10^{-6} bar. Directly after deposition the stamps were immersed in a suspension of βCD adsorbate in ethanol (1 mg in 20 ml). The procedure for the formation of the βCD SAM at a Au-coated PDMS stamp is slightly different from that reported for the βCD SAM preparation at Au solid substrates.[18] For solid substrates the βCD adsorbate is dissolved in an EtOH–$CHCl_3$ mixture due to the low solubility of the βCD adsorbate in EtOH. PDMS swells in chloroform, but only slightly in EtOH, and therefore ethanolic solutions of the adsorbate were used, since at 60 °C clear solutions could be obtained (1 mg per 20 ml). After immersion of the stamps in the βCD solutions at 60 °C for 16 h the stamps were removed from the warm solution and immersed in pure ethanol three times for 10 min and dried in a stream of N_2. The quality of the βCD SAM of the modified monolayer preparation was examined at solid substrates using contact angle measurements, cyclic voltammetry, heterogeneous electron transfer and electrochemical impedance spectroscopy, and the results were comparable to those found for the procedure for solid Au substrates.[18]

Water vapor was condensed at the βCD-functionalized, Au-coated stamps to enhance conformal contact between the stamp and the substrate by holding the stamp at a few cm distance for 5–8 s from water at 60 °C in a beaker.[42] The stamp was kept in conformal contact with the substrate for 3 h after which the stamp was removed and the metal film was left behind.

Electroless deposition of Cu

Electrochemical measurements were performed with an AUTOLAB PGSTAT10, in a custom built three-electrode setup equipped with a platinum counter electrode, a mercury sulfate reference electrode ($V_{MSE} = +0.61\ V_{NHE}$) and a screw cap holding the gold working electrode (area exposed to the solution = 0.44 cm^2). Electrodeposition was performed on the structures obtained by mTP in aqueous solution containing

10 mM Cu_2SO_4 and 10 mM H_2SO_4 at a static potential of -0.70 V_{MSE}.

Atomic force microscopy

AFM analyses were carried out with a Nanoscope III multimode AFM (Digital Instruments, Santa Barbara, CA, USA) with a J-scanner in contact mode using V-shaped Si_3N_4 cantilevers (Nanoprobes, Digital Instruments) with a spring constant of 0.1 N m^{-1}. Images were acquired in ambient atmosphere (relative humidity = 30–40% and $T = 25$ °C).

Optical microscopy

Optical micrographs were taken with an Olympus BH-2 microscope, equipped with CCD camera.

Electrical characterization

Electrical characterization of the devices was performed by current–voltage measurements using a Karl Süss PM8 Manual Probe station connected to a parameter analyzer (Agilent 4156B). Feather microneedles with a tip diameter of 5 μm were used to contact the structures under a N_2 atmosphere.

Acknowledgements

Dr Wilfred van der Wiel is gratefully acknowledged for fruitful discussions. The Dutch Technology Foundation STW is acknowledged for funding the Simon Stevin Award project on Nanolithography (Grant No. TST 4946 to D.N.R.).

References

1 (*a*) J. R. Sheatsa, *J. Mater. Res.*, 2004, **19**, 1974; (*b*) D. Braun and A. J. Heeger, *Appl. Phys. Lett.*, 1995, **66**, 2540.
2 (*a*) M. Granström, K. Petritsch, A. C. Arias, A. Lux, M. R. Andersson and R. H. Friend, *Nature*, 1998, **395**, 257; (*b*) C. J. Brabec, N. S. Sariciftci and J. C. Hummelen, *Adv. Funct. Mater.*, 2001, **11**, 15.
3 (*a*) H. E. Katz, Z. Bao and S. L. Gilat, *Acc. Chem. Res.*, 2001, **34**, 359; (*b*) Z. Bao, *Adv. Mater.*, 2000, **12**, 227.
4 C. P. Collier, G. Mattersteig, E. W. Wong, Y. Luo, K. Beverly, J. Sampaio, F. M. Raymo, J. F. Stoddart and J. R. Heath, *Science*, 2000, **289**, 1172.
5 A. R. Pease, J. O. Leppeson, J. F. Stoddart, Y. Luo, C. P. Collier and J. R. Heath, *Acc. Chem. Res.*, 2001, **34**, 433.
6 (*a*) S. Kubatkin, A. Danilov, M. Hjort, J. Cornil, J. L. Brédas, N. Stuhr-Hansen, P. Hedegård and T. Bjørnholm, *Nature*, 2003, **425**, 698; (*b*) J. Chen, M. A. Reed, A. M. Rawlett and J. M. Tour, *Science*, 1999, **286**, 1550.
7 L. H. Yu, Z. K. Keane, J. W. Ciszek, L. Cheng, M. P. Stewart, J. M. Tour and D. Natelson, *Phys. Rev. Lett.*, 2004, **93**, 266802.
8 (*a*) M. Geissler and Y. Xia, *Adv. Mater.*, 2004, **16**, 1249; (*b*) Y. Xia, J. A. Rogers, K. E. Paul and G. M. Whitesides, *Chem. Rev.*, 1999, **99**, 1823.
9 (*a*) J. L. Wilbur, A. Kumar, E. Kim and G. M. Whitesides, *Adv. Mater.*, 1994, **6**, 600; (*b*) R. J. Jackman, J. L. Wilbur and G. M. Whitesides, *Science*, 1995, **269**, 664.
10 H. Schmid, H. Wolf, R. Allenspach, H. Riel, S. Karg, B. Michel and E. Delamarche, *Adv. Funct. Mater.*, 2003, **13**, 145.
11 Y. L. Loo, R. L. Willett, K. W. Baldwin and J. A. Rogers, *Appl. Phys. Lett.*, 2002, **81**, 562.
12 Y. L. Loo, K. W. Baldwin and J. A. Rogers, *J. Am. Chem. Soc.*, 2002, **124**, 7654.
13 (*a*) Y. L. Loo, D. V. Lang, J. A. Rogers and J. W. P. Hsu, *Nano Lett.*, 2003, **3**, 913; (*b*) Y. L. Loo, J. W. P. Hsu, R. L. Willett, K. W. Baldwin, K. W. West and J. A. Rogers, *J. Vac. Sci. Technol., B*, 2002, **20**, 2853.
14 C. Kim, M. Shtein and S. R. Forrest, *Appl. Phys. Lett.*, 2002, **80**, 4051.
15 Y. L. Loo, R. L. Willett, K. W. Baldwin and J. A. Rogers, *Appl. Phys. Lett.*, 2002, **81**, 562.
16 (*a*) J. Zaumseil, M. A. Meitl, J. W. P. Hsu, B. R. Acharya, K. W. Baldwin, Y. L. Loo and J. A. Rogers, *Nano Lett.*, 2003, **3**, 1223; (*b*) S. Jeon, E. Menard, J. U. Park, J. Maria, M. A. Meitl and J. A. Rogers, *Adv. Mater.*, 2004, **16**, 1369.
17 (*a*) S. H. Hur, D. Y. Khang, C. Kocabas and J. A. Rogers, *Appl. Phys. Lett.*, 2004, **85**, 5730; (*b*) Z. Wang, J. Yuan, J. Zhang, R. Xing, D. Yan and Y. Han, *Adv. Mater.*, 2003, **15**, 1009.
18 (*a*) M. J. W. Beulen, J. Bügler, B. Lammerink, F. A. J. Geurts, E. M. E. F. Biemond, K. G. C. Leerdam, F. C. J. M. Van Veggel, J. F. J. Engbersen and D. N. Reinhoudt, *Langmuir*, 1998, **14**, 6424; (*b*) M. J. W. Beulen, J. Bügler, M. R. De Jong, B. Lammerink, J. Huskens, H. Schönherr, G. J. Vancso, B. A. Boukamp, H. Wieder, A. Offenhäuser, W. Knoll, F. C. J. M. Van Veggel and D. N. Reinhoudt, *Chem.-Eur. J.*, 2000, **6**, 1176.
19 S. Onclin, A. Mulder, B. J. Ravoo, J. Huskens and D. N. Reinhoudt, *Langmuir*, 2004, **20**, 5460.
20 T. Auletta, B. Dordi, A. Mulder, A. Sartori, S. Onclin, C. M. Bruinink, M. Péter, C. A. Nijhuis, H. Beijleveld, H. Schönherr, G. J. Vancso, A. Casnati, R. Ungaro, B. J. Ravoo, J. Huskens and D. N. Reinhoudt, *Angew. Chem., Int. Ed.*, 2004, **43**, 369.
21 (*a*) T. D. Tomalia, *Prog. Polym. Sci.*, 2005, **30**, 294; (*b*) A. W. Bosman, H. M. Janssen and E. W. Meijer, *Chem. Rev.*, 1999, **99**, 1665.
22 (*a*) J. F. G. A. Jansen, E. M. M. De Brabander-Van den Berg and E. W. Meijer, *Science*, 1994, **266**, 1226; (*b*) M. W. P. L. Baars, P. E. Froehling and E. W. Meijer, *Chem. Commun.*, 1997, 1959; (*c*) G. Pistolis, A. Malliaris, D. Tsiourvas and C. M. Paleos, *Chem.-Eur. J.*, 1999, **11**, 1440; (*d*) A. M. Naylor, W. A. Goddard III, G. E. Kiefer and D. A. Tomalia, *J. Am. Chem. Soc.*, 1989, **111**, 2339.
23 (*a*) J. J. Michels, J. Huskens and D. N. Reinhoudt, *J. Chem. Soc., Perkin Trans. 2*, 2002, 102; (*b*) R. M. Crooks, B. I. Lemon III, L. Sun, K. L. Yeung and M. Zhao, *Top. Curr. Chem.*, 2001, **212**, 81.
24 (*a*) M. C. Daniel, J. Ruiz, S. Nlate, J. C. Blais and D. Astruc, *J. Am. Chem. Soc.*, 2003, **125**, 2617; (*b*) W. Ong, M. Gomez-Kaifer and A. E. Kaifer, *Chem. Commun.*, 2004, 1677.
25 E. R. Gillies and J. M. J. Fréchet, *J. Am. Chem. Soc.*, 2002, **124**, 14137.
26 (*a*) R. W. J. Scott, O. M. Wilson, S. K. Oh, E. A. Kenik and R. M. Crooks, *J. Am. Chem. Soc.*, 2004, **126**, 15583; (*b*) M. Ooe, M. Murata, T. Mizugaki, K. Ebitani and K. Kaneda, *Nano Lett.*, 2002, **2**, 999.
27 A. M. Bittner, X. C. Wu and K. Klaus, *Adv. Funct. Mater.*, 2002, **12**, 432.
28 J. Huskens, M. A. Deij and D. N. Reinhoudt, *Angew. Chem., Int. Ed.*, 2002, **41**, 4467.
29 (*a*) C. A. Nijhuis, J. Huskens and D. N. Reinhoudt, *J. Am. Chem. Soc.*, 2004, **126**, 12266; (*b*) C. A. Nijhuis, Y. Fu, W. Knoll, J. Huskens and D. N. Reinhoudt, *Langmuir*, 2005, **21**, 7866.
30 C. A. Nijhuis, K. Dolatowska, B. J. Ravoo, J. Huskens and D. N. Reinhoudt, *Chem.-Eur. J.*, 2007, **13**, 69.
31 C. M. Bruinink, C. A. Nijhuis, M. Péter, B. Dordi, O. Crespo-Biel, T. A. Auletta, H. Schönherr, G. J. Vancso, J. Huskens and D. N. Reinhoudt, *Chem.-Eur. J.*, 2005, **11**, 3988.
32 (*a*) M. C. Daniel, J. Ruiz, S. Nlate, J. C. Blais and D. Astruc, *J. Am. Chem. Soc.*, 2003, **125**, 2678; (*b*) C. Valério, J. L. Fillaut, J. Ruiz, J. Guittard, J. C. Blais and D. Astruc, *J. Am. Chem. Soc.*, 1997, **119**, 2588; (*c*) M. C. Daniel, J. Ruiz, S. Nlate, J. C. Blais, N. Daro and D. Astruc, *Chem.-Eur. J.*, 2003, **9**, 4371.
33 (*a*) A. E. Kaifer, *Acc. Chem. Res.*, 1999, **32**, 62; (*b*) W. Ong, M. Gómez-Kaifer and A. E. Kaifer, *Chem. Commun.*, 2004, **15**, 1677.
34 (*a*) O. Crespo-Biel, B. Dordi, P. Maury, M. Peter, D. N. Reinhoudt and J. Huskens, *Chem. Mater.*, 2006, **18**, 2545; (*b*) O. Crespo-Biel, B. Dordi, D. N. Reinhoudt and J. Huskens, *J. Am. Chem. Soc.*, 2005, **127**, 7594.
35 C. A. Nijhuis, N. Oncel, J. Huskens, H. J. W. Zandvliet, B. J. Ravoo, B. Poelsema and D. N. Reinhoudt, *Small*, 2006, **2**, 1422.
36 H. Hillborg and U. W. Gedde, *IEEE Trans. Dielectr. Electr. Insul.*, 1999, **6**, 703.
37 S. H. Hur, D. Y. Khang, C. Kocabas and J. A. Rogers, *Appl. Phys. Lett.*, 2004, **85**, 5730.

38 N. Bowden, S. Brittain, A. G. Evans, J. W. Hutchinson and G. M. Whitesides, *Nature*, 1998, **393**, 146.
39 V. Zaporojtchenko, T. Strunskus, K. Behnke, C. Von Bechtolsheim, M. Kiene and F. Faubel, *J. Adhes. Sci. Technol.*, 2000, **14**, 467.
40 G. C. Martin, T. T. Su, I. H. Loh, E. Balizer, S. T. Kowel and P. Kornreich, *J. Appl. Phys.*, 1982, **53**, 797.
41 The nomenclature for dendrimer generations as described in T. D. Tomalia, A. M. Naylor and W. A. Goddart, III, *Angew. Chem., Int. Ed. Engl.*, 1990, **29**, 144, is generally applied for PAMAM dendrimers. However, a different system for PPI dendrimers starting at G1 is common in the literature. Thus, a G0-PAMAM dendrimer has 4 end groups and a G1-PAMAM dendrimer has 8, while a G1-PPI dendrimerhas 4 end groups and a G2-PPI dendrimer has 8, *etc.*
42 S. Hoeppener, R. Maoz and J. Sagiv, *Nano Lett.*, 2003, **3**, 761.
43 Special edition on cyclodextrins: V. T. D'Souza and K. B. Lipkowiz, *Chem. Rev.*, 1998, **98**, 1741.
44 The presence of water is also crucial to the electronic properties of the junctions: in ref. 35, Coulomb blockade behavior was observed of dendrimers loaded with a Au nanoparticle adsorbed at the molecular printboard only by STM under *ambient* conditions and not under ultra high vacuum conditions.
45 J. Huskens, A. Mulder, T. Auletta, C. A. Nijhuis, M. J. W. Ludden and D. N. Reinhoudt, *J. Am. Chem. Soc.*, 2004, **126**, 6784.
46 (*a*) E. A. Speets, B. J. Ravoo, F. J. G. Roesthuis, F. Vroegindeweij, D. H. A. Blank and D. N. Reinhoudt, *Nano Lett.*, 2004, **4**, 841; (*b*) J. A. M. Sondag-Huethorst and L. G. J. Fokkink, *Langmuir*, 1995, **11**, 4823.
47 (*a*) Y. Xia and G. M. Whitesides, *Angew. Chem., Int. Ed.*, 1998, **37**, 550; (*b*) Y. Xia, X. M. Zhao, E. Kim and G. M. Whitesides, *Chem. Mater.*, 1995, **7**, 2332.
48 (*a*) J. Chen, M. A. Reed, A. M. Rawlett and J. M. Tour, *Science*, 1999, **286**, 1550; (*b*) Y. Xue, S. Datta, S. Hong, R. Reifenberger, J. I. Henderson and C. P. Kubiak, *Phys. Rev. B: Condens. Matter Mater. Phys.*, 1999, **59**, R7852; (*c*) S. I. Khondaker, Y. Zhen, L. Cheng, J. C. Henderson, Y. Yao and J. M. Tour, *Appl. Phys. Lett.*, 2004, **85**, 645; (*d*) N. Gergel, N. Majumdar, K. Keyvanfar, N. Swami, L. R. Harriott, J. C. Bean, G. Pattanaik, G. Zangari, Y. Yao and J. M Tour, *J. Vac. Sci. Technol., A*, 2005, **23**, 880.
49 C. B. Gorman, R. L. Carroll and R. R. Fuierer, *Langmuir*, 2001, **17**, 6923.
50 A. V. Tivanski and G. C Walker, *J. Am. Chem. Soc.*, 2005, **127**, 7647.
51 R. A. Wassel, G. C. Credo, R. R. Fuierer, D. L. Feldheim and C. B. Gorman, *J. Am. Chem. Soc.*, 2004, **126**, 295.
52 J. He and S. M. Lindsay, *J. Am. Chem. Soc.*, 2005, **127**, 11932.
53 P. R. Ashton, R. Königer, J. F. Stoddart, D. Alker and V. D. Harding, *J. Org. Chem.*, 1996, **61**, 903.
54 I. Cuadrado, M. Morán, C. M. Casado, B. Alonso, F. Lobete, B. García, M. Ibisate and J. Losada, *Organometallics*, 1996, **15**, 5278.
55 M. W. P. L. Baars, A. J. Karlsson, V. Sorokin, B. F. W. De Waal and E. W. Meijer, *Angew. Chem., Int. Ed.*, 2000, **39**, 4262.